

The evolution of African monsoons and its impacts on precipitation seasonality in the late Cenozoic and future climate change



Daniel Boateng¹, Frank Arthur², Michael Baidu³, Jeffrey N. A. Aryee⁴

¹Department of Geosciences, University of Tübingen, Germany; ²Department of Natural Sciences and Environmental Health, University of South-Eastern Norway, Bø, Norway; ³Institute of Climate and Atmospheric Science, School of Earth and Environment, University of Leeds; ⁴Department of Meteorology and Climate Science, Kwame Nkrumah University of Science and Technology, Kumasi, Ghana



1 Introduction

The West African Monsoon (WAM) strongly drives precipitation variability and seasonality across continental West Africa and the tropical Eastern Atlantic. However, the evolution of the WAM in the late Cenozoic, in response to changes in vegetation, atmospheric CO₂, orbital forcings, paleogeography, and orography as well as its teleconnections such as the mean location of the African Easterly Jet (AEJ), Tropical Easterly Jet (TEJ), Sub-Tropical Jet (STJ), Inter-Tropical Discontinuity (ITD) and low-level westerly flow is not well constrained. We contribute to understanding past WAM dynamics by performing high-resolution, time-specific paleoclimate simulation using General Circulation Model ECHAM5. We focus our analysis on the migration and intensification of the WAM and its associated atmospheric thermodynamic structure which influence the rainfall seasonality and patterns across the Sahel, Guinea Coast, and Sahara regions.

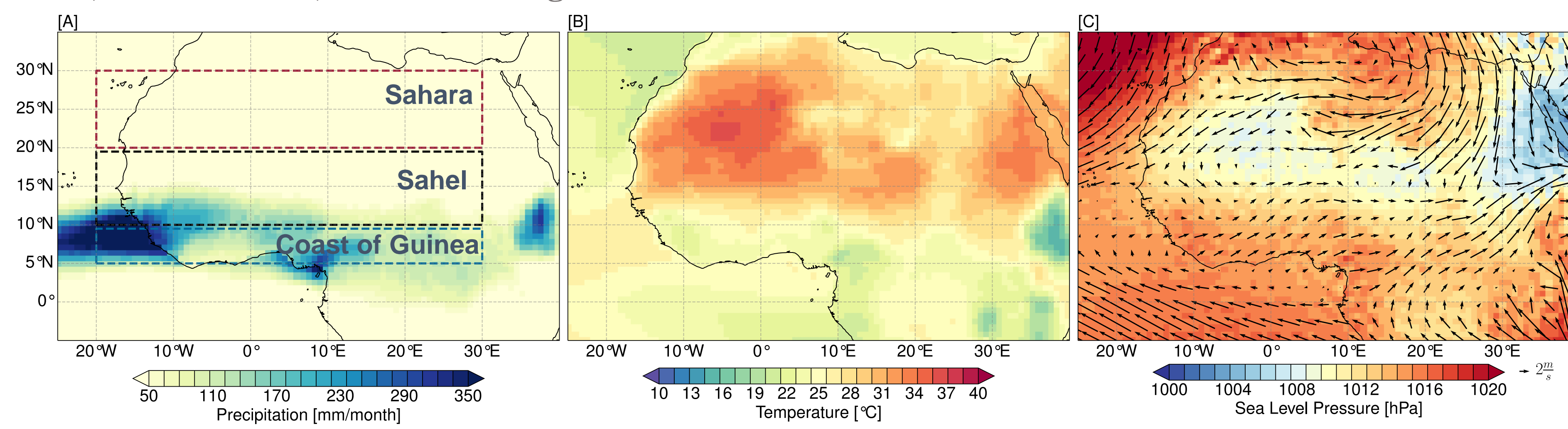
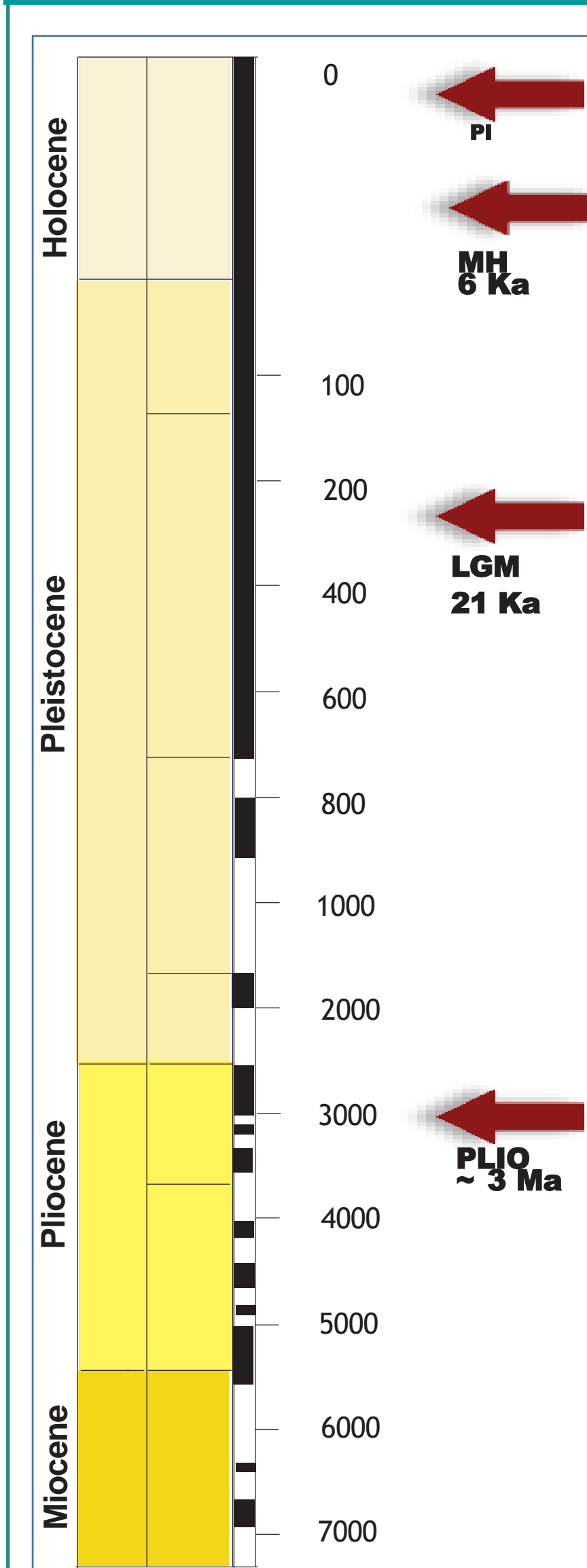


Fig. 1: Annual climatological means of June-July-August-September (JJAS) months for (a) total precipitation amount, (b) near-surface temperature, and (c) mean sea level pressure (background) and wind shear at 850 hPa (arrows) for the Pre-Industrial (PI) simulation. The PI climatologies are highly comparable to present-day climate patterns during the WAM season, constraining the tropical rain belt to the south of the Sahara heat low.

2 Methods



We use the global Atmospheric GCM ECHAM5 (MPI, Hamburg); resolution T159 (ca. 80km x 80km) with 31 vertical levels, 6h temporal resolution outputs.

Pre-industrial (PI): standard protocol Atmospheric Model Intercomparison Project (AMIP2)-style PI experiment (Taylor et al. 2000); SST and SIC derived from transient coupled ocean-atmosphere run (Lorenz and Lohmann 2004; Dietrich et al. 2011). GHG concentrations (Dietrich et al. 2013): CO₂ 280 ppm, CH₄ 760 ppm, and N₂O 270 ppm.

Mid Holocene (MH): SST & SIC derived from low-resolution, coupled atmosphere-ocean transient Holocene run (Wei and Lohmann, 2012). GHG concentrations (Dietrich et al. 2013): CO₂ 280 ppm, CH₄ 650 ppm, and N₂O 270 ppm.

Last Glacial Maximum (LGM): SST & SIC based on reconstructions from the GLAMAP (Sarnthein et al., 2003). GHG concentrations: CO 185 ppm, CH 350 ppb, and N₂O 200 ppb.

Pliocene (PLIO): boundary conditions from the PRISM (Pliocene Research, Interpretation and Synoptic Mapping) project. Vegetation from the PRISM vegetation reconstructed to the JSBACH plant functional types (Stepanek and Lohmann 2012), GHG concentrations: CO₂ 405 ppm.

References



3 Results

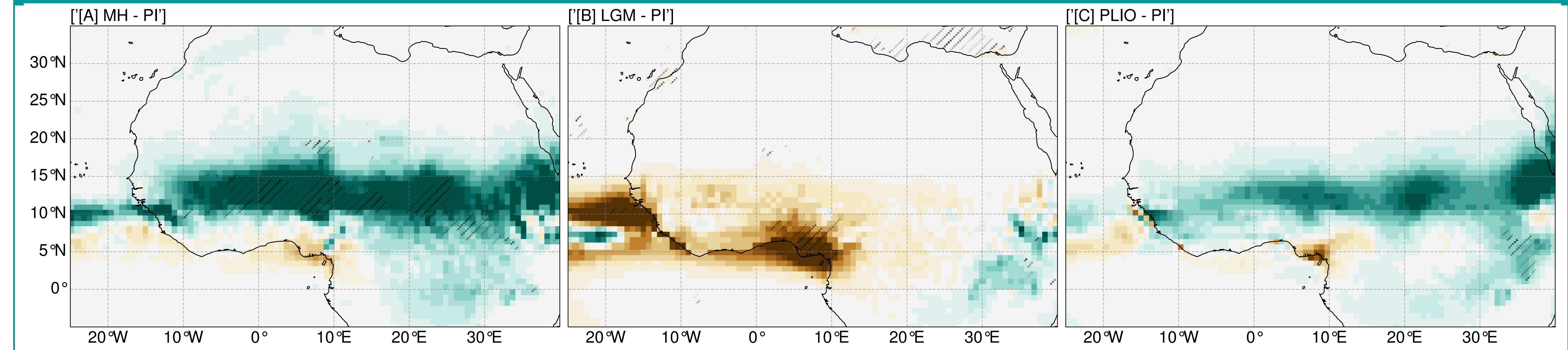


Fig. 2: Annual mean climatological difference for JJAS for precipitation in response to (a) MH (b) LGM, and PLIO paleoenvironment conditions.

Figure 3 shows three maps of West Africa and the Eastern Atlantic, labeled (A) MH - PI, (B) LGM - PI, and (C) PLIO - PI. These maps display the annual mean climatological difference in precipitation (mm/month) for the JJAS season. A color scale at the bottom ranges from -150 to 150 mm/month, with blue indicating negative differences and red indicating positive differences. Map (A) shows a significant positive difference (wetter conditions) across the Sahel and Guinea Coast. Map (B) shows a large negative difference (drier conditions) across the entire region. Map (C) shows a positive difference, particularly in the Sahel and Guinea Coast, but with some negative differences in the Sahara.

Fig. 3: Annual mean climatological difference for JJAS for near-surface temperature in response to (a) MH (b) LGM, and PLIO paleoenvironment

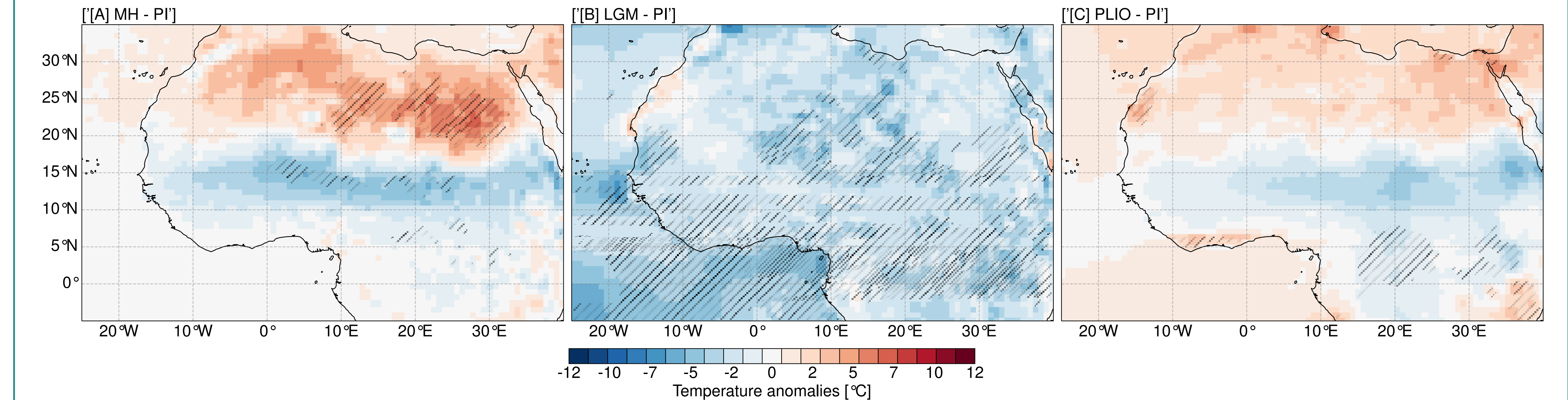


Fig. 4: Monthly precipitation patterns simulated from the PI (black), MH (red), LGM (blue), and PLIO (green) paleoenvironment conditions across the (a) Sahara, (b) Sahel, and (c) Guinea Coast.

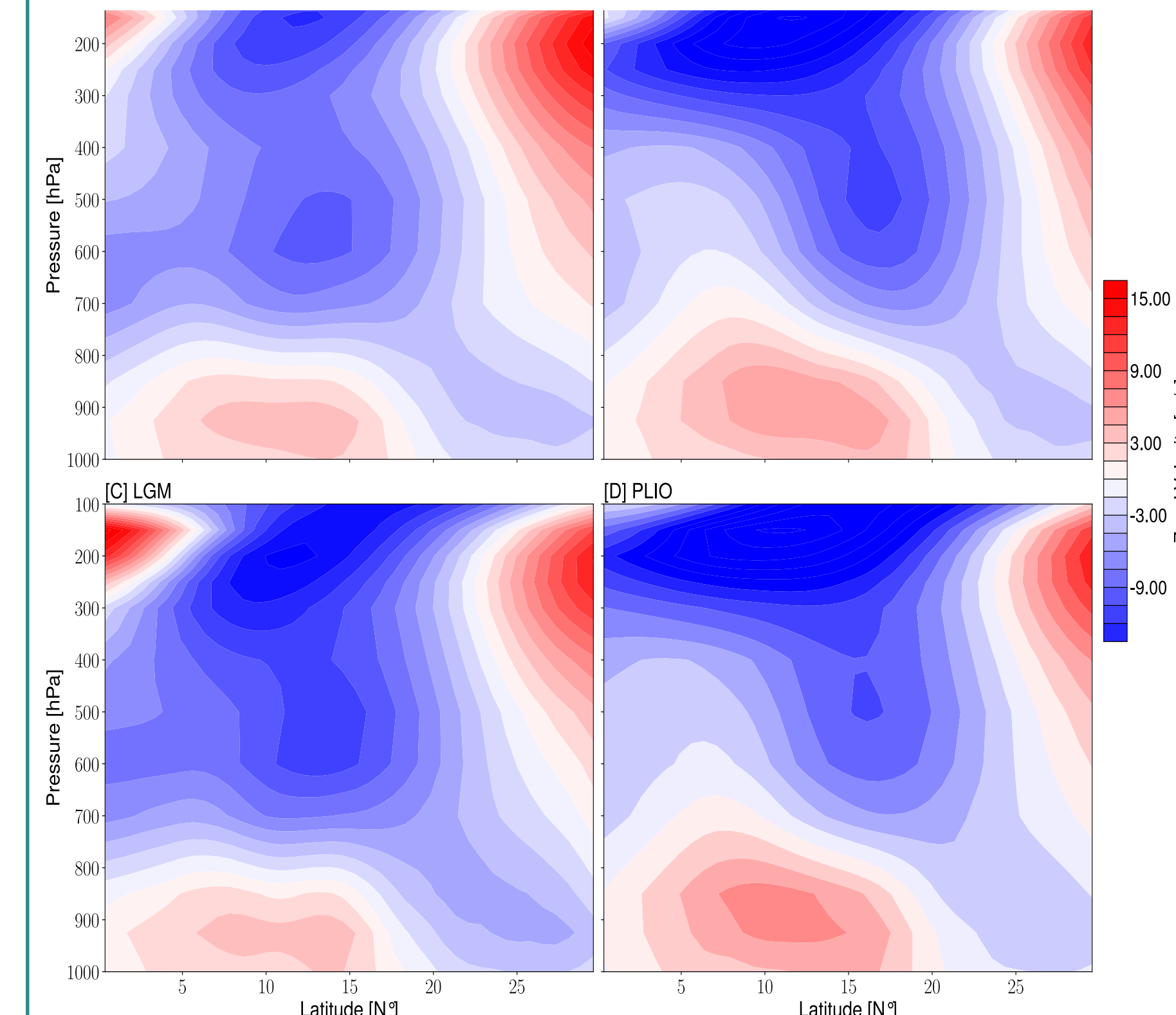


Fig. 5: Pressure-Latitude cross-sectional patterns of zonal wind speeds (m/s) from the (a) PI, (b) MH, (c) LGM, and (d) PLIO paleoclimatic regimes showing the monsoon depth, AEJ, TEJ, and STJ locations.

4 Summary and Conclusion

The simulated climate patterns in the PI are reasonably comparable to the present-day patterns during the WAM season, constraining the tropical rain belt to the south of the Saharan Heat Low. The MH and PLIO simulate wetter conditions and increase in the northward extent due to deeper monsoon depth, stronger TEJ, and pronounce meridional temperature gradient compared to the PI. The LGM simulates extensive dry conditions across the continent due to overall spatial cooling.

